Biomedical Physics & Engineering Express

PAPER

Optimizing 3D-printed workpieces for radiotherapy application: modelling the CT number and print time

RECEIVED
19 October 2023

REVISED
19 December 2023

ACCEPTED FOR PUBLICATION
8 January 2024

PUBLISHED
18 January 2024

Sehad Kadiri[1], **Kaltrine Jakupi**[2,3], **Vladimir Dukovski**[3] and **Gezim Hodolli**[4]

[1] Faculty of Radiology, AAB College, 10000 Pristina, Kosovo
[2] Faculty of Mechanical Engineering, University of Pristina 'Hasan Prishtina', 10000 Pristina, Kosovo
[3] Faculty of Mechanical Engineering, 'Ss. Cyril and Methodius' University in Skopje, 1001 Skopje, North Macedonia
[4] Faculty of Veterinary and Agriculture, University of Pristina 'Hasan Prishtina', 10000 Pristina, Kosovo

E-mail: kaltrine.jakupi@uni-pr.edu

Keywords: 3D, PLA, electron density, radiotherapy, optimizing

Abstract

This study aims to analyze the influence of specific printing parameters, including infilling, print speed, and layer height, on the CT numbers and printing time of 3D-printed workpieces fabricated from Polylactic Acid (PLA). The primary objective is to optimize these parameters to attain desired CT numbers and print time for radiotherapy applications. To achieve this objective, we employed the Taguchi experimental design and regression analysis methodologies. A series of experiments were conducted to systematically assess the effects of varying infilling, print speed, and layer height values on the CT numbers and printing time of the PLA workpieces. The resulting data were then used to create mathematical models for predicting optimal parameter settings. Our investigations revealed that specific adjustments to infilling and layer height significantly influence the CT numbers and printing time of 3D-printed workpieces. By leveraging the developed mathematical models, precise predictions can be made to optimize independent parameters for the desired CT numbers and printing times, enhancing the efficacy of 3D-printed workpieces for radiotherapy applications. This research contributes to the advancement of 3D-printed workpieces utilized in radiotherapy, offering a pathway to enhance the accuracy and efficiency of treatment delivery. The optimization of printing parameters outlined in this study provides a valuable tool for clinicians and researchers in the field, ultimately benefiting patients undergoing radiotherapy treatments.

1. Introduction

Additive manufacturing (AM), also known as 3D printing, has rapidly emerged as a disruptive manufacturing technology that enables the production of complex geometries with high precision and customization. Unlike traditional manufacturing techniques that rely on subtractive or formative processes, additive manufacturing builds parts layer by layer from digital designs. This approach offers several advantages, including faster prototyping, reduced material waste, and improved design freedom [1]. The rapid growth and diverse applications of additive manufacturing have fueled research and development efforts to improve the technology, materials, and processes involved. This has led to advancements in 3D printing technology, including the development of new materials, process monitoring, and post-processing techniques [2].

AM has emerged as a powerful tool in the field of medicine, enabling the production of complex and customized medical devices and implants. AM has been used to produce patient-specific prosthetics, surgical guides, and implants, which can be customized to match the patient's anatomy and improve the precision and accuracy of surgical [3].

Radiotherapy is a common treatment modality for cancer patients, and accurate dose delivery to the tumor is crucial for successful outcomes. One way to improve the accuracy of dose delivery is through the use of boluses, which are materials placed on or near the patient's skin to modify the dose distribution of the radiation beam. They are used to compensate for irregularities in the patient's anatomy, provide tissue equivalent buildup, or create a more uniform dose distribution. In addition to commercial boluses, patient personalized boluses manufactured with a 3D printer

© 2024 IOP Publishing Ltd

have lately found application due to its benefits on better dose distribution [4]. The skin sparing effect is caused by high energy photon beams with a low dose at the skin surface [5]. With the advent of 3D printing technology, it is now possible to create patient-specific boluses that can improve dose conformity and reduce treatment time compared to traditional boluses [4].

The attenuation coefficient of an x-ray beam passing through a material is influenced mainly by Electron Density (ED) of material. The ED refers to the number of electrons per unit volume in a specific tissue or material. Materials with higher electron densities, such as bone or metals, have higher attenuation coefficients compared to materials with lower electron densities, such as air or water. Therefore, the ED of the materials used to print the 3D boluses is crucial parameter in radiotherapy for treatment planning, as it is used to calculate the dose distribution and determine the accuracy of the treatment. There are also some other parameters [5, 6], which influenced the attenuation coefficient but are kept constant on this study.

The Hounsfield unit (HU) is a unit of measurement used in computed tomography (CT) imaging to quantify the radio density of different tissues [7]. The relationship between the HU and ED is not a linear one. The HU scale is primarily based on the linear attenuation coefficients of different materials relative to water and air.

In general, materials with higher ED tend to have higher HU values, indicating increased radio density on CT images. For example, bone has a higher electron density than soft tissues, and thus it appears more radio dense on CT scans, corresponding to higher HU values. Similarly, metals or dense foreign bodies can have very high HU values due to their high electron densities.

The HU scale is based on the radio density of water (assigned a value of 0 HU) and air (assigned a value of −1000 HU). Other materials, such as bone, have higher positive HU values due to their higher density and greater x-ray attenuation.

HU values obtained from CT scans are used to assign specific electron densities to tissues during radiotherapy treatment planning. Conversion tables or calibration curves are employed to convert HU values to corresponding electron density values. By correlating HU values to electron density, the treatment planning system can accurately calculate the radiation dose distribution within the patient's body. For more details of relationship between HU and ED can be found elsewhere [8–10].

The Hounsfield Unit (HU) scale encompasses a range of CT numbers, from −1000 HU for dry air to 1000 HU for compact bone. Ideally, water is assigned a CT number value of 0 HU. Consequently, any material with an attenuation slightly higher (approximately 0.1%) than that of water will exhibit a HU value of 1.

In summary, both ED and HU play significant roles in radiotherapy treatment planning using CT simulators. ED provides essential information about the tissue composition and its interaction with radiation, while HU derived from CT scans serve as a basis for converting radio density values to ED during the treatment planning process.

Table 1. The combination of independent parameters and dependent parameters.

Nr	Independent/Input parameters			Dependent parameters	
	I - Infill percentage (%)	PS - Print Speed (mm/s)	LH - Layer Height (mm)	CT number (HU)	Printing time (min)
1	50	40	0.13	−312	106
2	50	70	0.19	−222	73
3	50	100	0.25	−130	56
4	75	40	0.19	−110	80
5	75	70	0.25	−13	58
6	75	100	0.13	−84	111
7	100	40	0.25	92	76
8	100	70	0.13	129	116
9	100	100	0.19	145	80

The Polylactic acid (PLA) thermoplastic is a popular material for 3D printing of boluses [11, 12] due to its biocompatibility, ease of use, and availability. The PLA is a biodegradable and biocompatible thermoplastic that has found widespread use in the field of additive manufacturing due to its ease of printing, low cost, and sustainability [13].The aim of this study is to verify whether 3D-printed boluses can be produced from PLA (Polylactic Acid) material, which will have the ability to modify dose distribution based on printing parameters. Additionally, the purpose of this study is to determine the function and level of influence of printing parameters, such as infilling, print speed, and layer height, on the Hounsfield Unit (HU) values. Recent literature explores 3D printing in radiotherapy, but a gap exists in optimizing parameters like CT number and print time. Addressing this is crucial for precise tissue representation and efficient printing, advancing the customization of 3D-printed models in radiotherapy planning.

2. Material and methods

2.1. Design of experiment

To optimize the printing parameters of 3D printed workpieces made by PLA material and investigation of their effects on the CT numbers (HU), the Taguchi statistical method was used [14]. It reduces the number of experiments and at the same time do not reduce the quality of conclusions. For three input printing parameters: infilling percentage, printing speed, and layer thickness, within specific ranges of (50, 75, and 100%), (40, 70, and 100 mm s^{-1}), and (0.13, 0.19, and

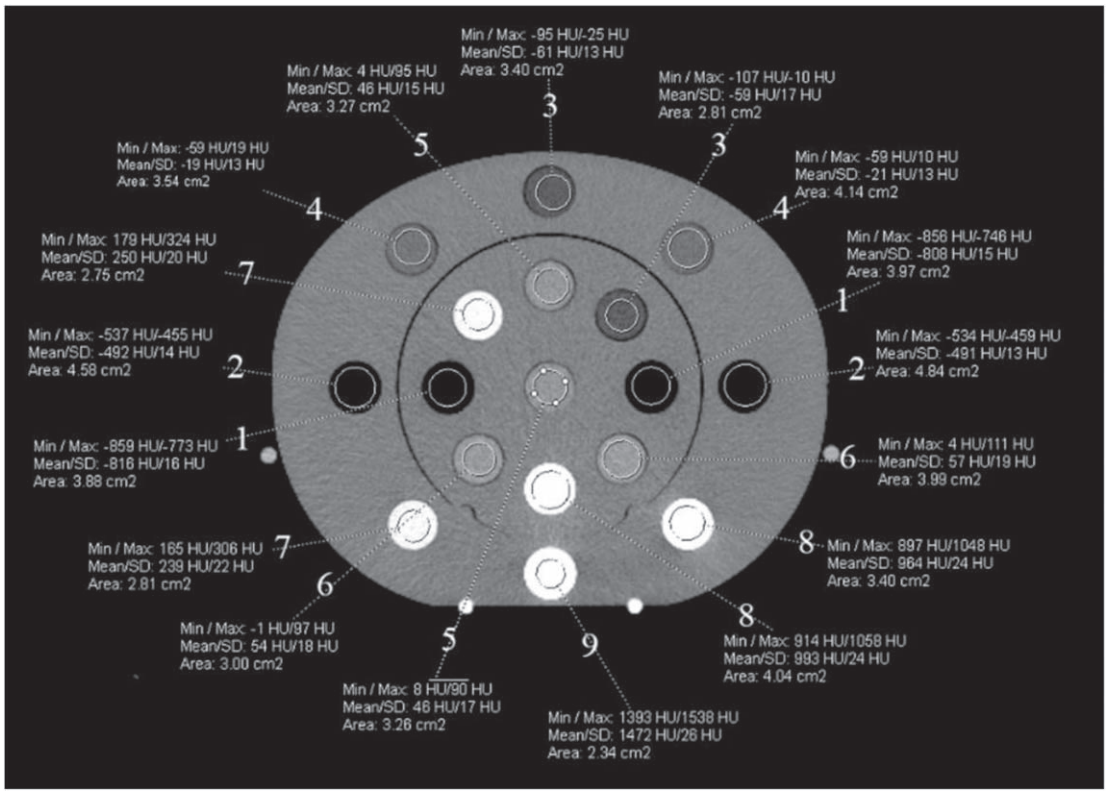


Figure 1. CT numbers of electron density phantom model 064 M (3rd measurement).

0.25 mm), respectively. The workpieces were designed by PrusaSlicer software, version 2.6.0. The workpieces were designed as cylindrical shape with diameter of 2 cm and the height 5 cm. same shape and volume of workpieces were used for all nine experiments but input parameters were presented on table 1, specific with printing time of each workpieces. The process of design and production were explained elsewhere [15].

The commercial 3D printer were used to print the designed object by PLA thermoplastic material with filament diameter 1.75 mm. The printer was calibrated in accordance with the manufacturer's instructions. The printer set up were: nozzle diameter 0.4 mm, extruder temperature were 200 °C, the bed printing temperatures were 60 °C.

2.2. CT simulation

The CT Simulator, specifically the Siemens GoSim model with 32 slices, was employed to perform scans on the Electron Density Phantom model 062 M. This phantom is equipped with tissue electron density rods and adheres to the criteria outlined in TG 66 of the American Association of Physicists in Medicine (AAPM) [16] and ICRU44 [17]. Additionally, nine 3D printed workpieces were scanned using the same scanning parameters on the CT Simulator.

2.3. Theoretical modelling

In this study, the multiple regression analysis was applied to investigate the relationship between the input printing parameters and the HU of 3D printed workpieces. Multiple regression analysis has been widely used in previous studies for establishing relationships between dependent and independent variables. The independent variables in this study were chosen based on their potential influence on HU, including infilling percentage, printing speed, and layer thickness. The dependent variable, HU, can be expressed as an linear function of the independent variables. The least squares approach was used to estimate the exponential coefficients of equation.

3. Results and discussions

3.1. Calibration curve for relation of ED versus CT numbers

To find the calibration curve, we performed CT scans of the Electron Density Phantom Model 062 M. This phantom contains various standard tissue substitute materials with known densities. Figure 1 displays the CT numbers for nine different tissue substitute materials of scanned phantom.. For quality control and statistical reasons the same phantom with all identical scanning parameters were scanned three times. The measurements of CT numbers for each substitute plugs with each specific ED are represented on table 2. An accurate calibration curve (figure 2) was constructed by utilizing certified electron densities obtained from phantom certification and their corresponding

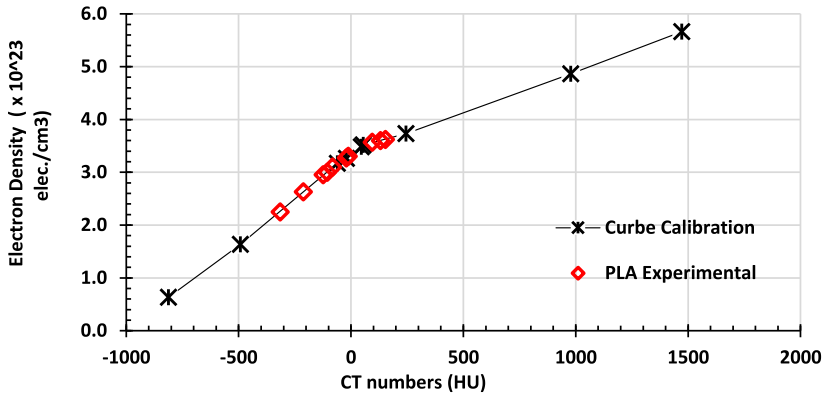


Figure 2. The calibration curve of CT number and ED.

Table 2. CT numbers for each tissue substitute materials, from Phantom 062 M.

No.	Tissue substitute material	ED x 10^{23} (electrons/cm^3)	CT numbers (HU), N = 3		
			1	2	3
1	Lung Inhale	0.634	−816	−808	−812.0
2	Lung Exhale	1.632	−492	−491	−491.5
3	Adipose	3.171	−61	−59	−60.0
4	Breast 50/50	3.261	−19	−21	−20.0
5	Muscle	3.483	46	46	46.0
6	Liver	3.516	54	57	55.5
7	Bones 200 mg	3.730	239	250	244.5
8	Bone 800 mg	4.862	964	993	978.5
9	Bone 1250 mg	5.663	1472	1472	1472.0

measured CT numbers. The extreme CT numbers were measured for lung and bone (1250 mg), −816 and 5,663 HU, respectively, correspond to electron densities of 0.634 and 5,663 × 10^{23} electron/cm^3, respectively. The mean CT numbers (HU) and corresponding standard deviation (SD) values for each material are presented in table 2.

Once the calibration curve is established, the HU of the phantom material can be measured and converted to electron density using the equation:

$$ED = \frac{HU - HU_{water}}{HU_{water} - HU_{air}}\rho_{water} \quad (1)$$

Where: ρ water is the electron density of water, HUwater is the HU of water, HUair is the HU of air, and HU is the HU of the phantom material [18].

The black line on the figure 2, represents the calibration curve, with black markers displaying the results obtained from the phantom, while nine red markers represent the ratio of CT numbers of scanned printed workpieces to their specific electron densities. Through this curve, the possibility to convert HU of scanned materials to ED was created.

The CT numbers were determined through the CT simulation of workpieces composed of PLA material (figure 3).

3.2. CT Simulation of printed workpieces

The CT simulation of the printed workpieces were done in accordance with protocol used for the Electron Density Phantom CT simulation. Figure 3 shows sectional view of 12 workpieces, printed in accordance with indepedent parameters specified on table 1. Additionally, three extra workpieces labeled A, B, and C were created. These workpieces were printed with randomly choosen independent variables: infilling of 50%, 75%, and 100%; print speeds of 70, 70, and 100 mm s^{-1}; and layer heights of 0.19, 0.25, and 0.25 mm for workpieces A, B, and C, respectively.

3.3. Theoretical models of CT numbers and HU.

The dependent variables of CT numbers and print times are presented on the table 1, those variables were measured for each printed workpiece, while adhering to the specified values of the independent parameters as recommended by the Taguchi method. Using the regression method for linear mathematical functions, we have derived two equations that calculate the value of the dependent parameter, either the CT number or the printing time, for any given combination of independent parameter values. These equations are as follows:

$$CT_{nr} = -786,61 + 6,87 * I + 1,5 * P + 600 * H \quad (2)$$

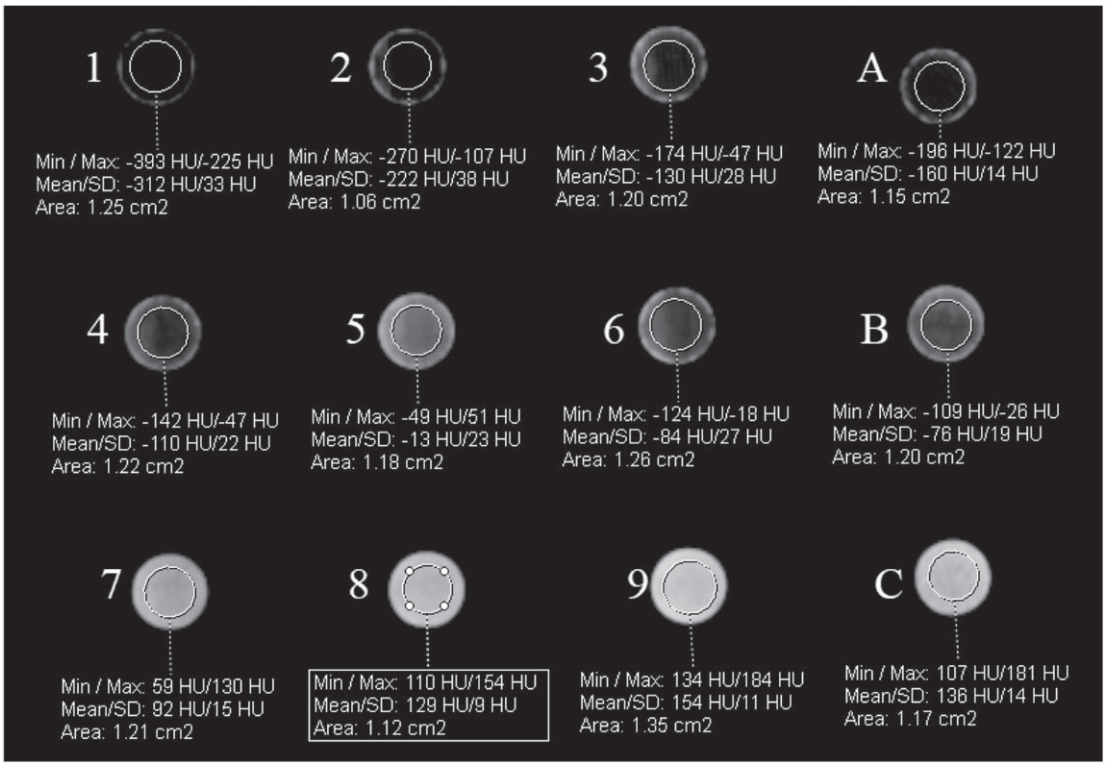


Figure 3. CT simulation of printed workpieces.

Table 3. Comparisons of measured and calculated values for dependent parameters.

Nr	Independent parameters			Dependent parameters			
				CT numbers		Print Time	
	Infilling (%)	Print speed (mm/s)	Layer Height (mm)	Measured (HU)	Calculated (HU)	Measured (min)	Calculated (min)
A	50	70	0.25	−160	−191.81	56	54.02
B	75	70	0.19	−76	−56.16	76	84.03
C	100	100	0.25	136	194.99	62	63.87

$$P_{rint} = 146,81 + 0,25 * I - 0,08 * P - 397.22 * H \quad (3)$$

Where: CTnumber—Presents the value of scanned workpieces in HU unit, Print time—presents the time needs to print specific workpieces in minutes, I—Infilling(%), P—print speed (mm/s) and H—Height (mm).

From summary output of nine observations, the main statistical parameter of regression method are: R Square: 0.98 and 0.94, Adjusted R Square: 0.96 and 0.90, standard error: 30.7 and 6.93, for CT numbers and Print Time, respectively. Also, both models fulfill ANOVA criteria for quality of models, the alpha values are 0.0002 and 0.002 for CT number and Print time models, respectively.

Table 3 displays the values of the dependent parameters (Infilling, print speed, and layer height) that were used to print workpieces A, B, and C. These specific parameters were chosen arbitrarily. In the second part of the same table, the results of the dependent parameters (CT numbers and- print time) are presented, for which the measured and calculated values using equations 3 and 4 were found, respectively, for CT number and print time.

The average ratio of theoretical values compared to experimental values for CT number and print time is 1.12 and 1.03, respectively. Therefore, in conclusion, we can say that the theoretical models expressed by equations (2) and (3) have reasonable accuracy to be used for calculation of the dependent parameters for any given combination of independent parameters.

3.4. Assessing independent parameter significance in CT numbers and print time

To assess the impact of independent parameters (infilling, print speed, and layer height) on dependent parameters (CT numbers and printing time), we have determined the average values of independent

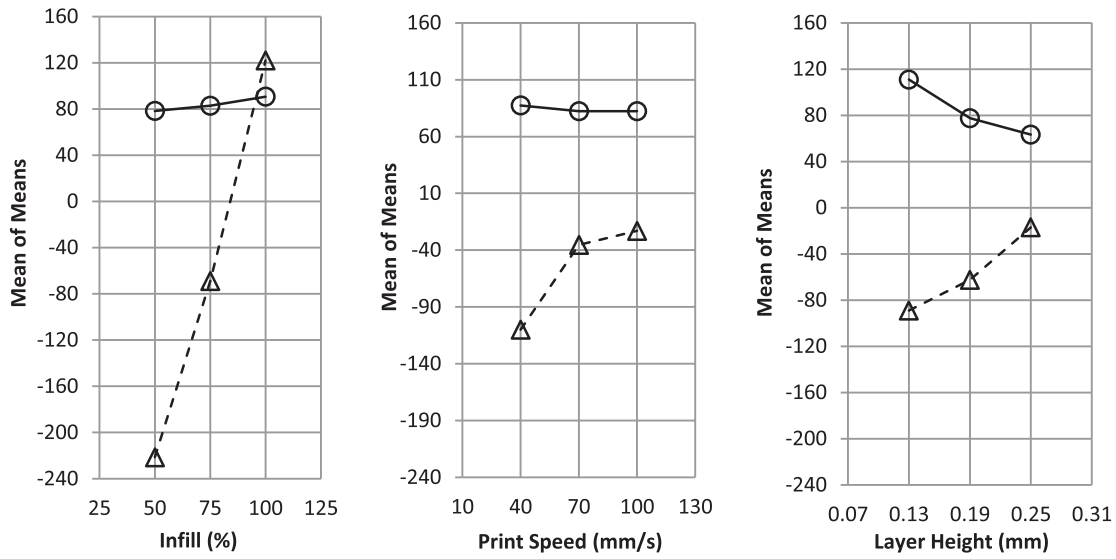


Figure 4. Main effect of mean for each indepedent parameters related to CT numbers and Print time (Legende: The CT numbers are expressed by dashed lines with triangle markers. The printing time are expressed by solid line with circled markers).

parameters for each value of dependent parameters from table 1. Figure 4 illustrates the graphs of the three independent parameters and their effects on the dependent parameters.

The primary objective in radiotherapy is to produce boluses that enable the highest possible radiation dose, particularly in close proximity to the skin. This can be achieved by ensuring that the CT numbers of the boluses are as high as possible. However, increasing the CT numbers also leads to an increase in the printing time of the bolus. Ideally, we would like to find the combination of independent parameters that would create a bolus with highest CT number and a shortest of printing time. To achieve this goal, we utilized theoretical models expressed by equations 3 and 4.

To better visualize the impact of the independent parameters, figure 4 has been constructed, based on experimental data, illustrating how the values of each independent parameter (Infilling, Print speed, or Layer Height) relate to the mean of mean values for CT number (indicated by dashed lines with triangle markers) and printing time (indicated by a solid line with circled markers).

Infill: Among all the parameters in this study, this particular independent parameter holds the highest degree of significance. As observed in the first graph of figure 4, increasing the infill percentage is directly associated with an increase of the CT number values, aligning with our intended goal. However, it's noteworthy that this increment in the infill percentage also leads to a subsequent increase in the printing time. Both the graphical representation and the theoretical models demonstrate a noteworthy rate of increase in CT numbers compared to printing time. Consequently, we can confidently conclude that elevating the infilling parameter favors the creation of a bolus with the desired characteristics.

Print Speed: Additionally, as observed in the second graph of figure 4, increasing the print speed results in higher CT number values, while also easily attaining shorter printing times for the printed components. Layer Height: The third graph in figure 4 illustrates that increasing the layer height leads to higher CT number values and a reduction in printing time. The rate of change for both models is almost identical but with opposite trends. Consequently, it is advisable for this parameter to have higher values when printing components intended for use as boluses in radiotherapy.

The research findings suggest the potential for constructing workpieces using a 3D printer, allowing manipulation of CT number values and simultaneous estimation of printing time based on printing parameters. The generated models enhance precision in determining CT number and printing time prior to initiation printing.

Utilizing the empirical findings of this study, practitioners in the field of radiotherapy will possess preliminary insights into the impact of radiation distribution and the temporal parameters related to the fabrication of various workpieces. Consequently, they will be equipped with antecedent knowledge pertaining to the anticipated scenarios they may encounter.

4. Conclusion

In the context of radiotherapy applications, the utilization of 3D-printed components is steadily on the rise. These printed components, tailored especially for patients, can facilitate the attainment of the desired dose delivery. The electron density of these workpieces stands out as a pivotal factor influencing dose distribution.

In this study, were employed PLA material to print workpieces. These workpieces were used to investigate the influence of independent parameters (infilling,

print speed, and layer height) on the values of CT numbers and printing time. The theoretical models developed for CT numbers and print time of workpieces demonstrate a satisfactory level of accuracy and can be effectively employed to calculate outcomes for various combinations of independent parameters.

To attain a substantial electron density within a 3D-printed workpieces for radiotherapy purposes, it is advisable, as per the insights derived from this study, to opt for a high infill percentage and a greater layer height. A high infill percentage guarantees the absence of voids within the component, while an increased layer height substantially minimizes printing time. Moreover, the print speed exhibits a favorable influence on elevating the CT number and reducing print time; however, it is prudent to maintain it within an optimal range to mitigate the risk of printing failures.

Data availability statement

The data cannot bemade publicly available upon publication because they are not available in a format that is sufficiently accessible or reusable by other researchers. The data that support the findings of this study are available upon reasonable request from the authors.

ORCID iDs

Sehad Kadiri https://orcid.org/0000-0002-6986-9842
Kaltrine Jakupi https://orcid.org/0000-0003-1340-1375
Vladimir Dukovski https://orcid.org/0000-0002-9033-8923
Gezim Hodolli https://orcid.org/0000-0002-5107-6481

References

[1] Gibson I, Rosen D W and Stucker B 2010 Additive Manufacturing Technologies *Rapid Prototyping to Direct Digital Manufacturing* (Springer) XXII, 459
[2] Bikas H, Stavropoulos P and Chryssolouris G 2016 Additive manufacturing methods and modelling approaches: a critical review *Int. J. Adv. Manuf. Technol.* **83** 389–405
[3] Lal H and Patralekh M K 2018 3D printing and its applications in orthopaedic trauma: a technological marvel *J. Clin. Orthop. Trauma.* **9** 260–8
[4] Jakupi K, Vrtanoski G, Dukovski V and Hodolli G 2022 Design and manufacturing of 3d printed parts for radiotherapy application **40** 11–5
[5] Kastrati L *et al* 2021 Applications and benefits of using gradient percentage depth dose instead of percentage depth dose for electron and photon beams in radiotherapy *Pol. J. Med. Phys. Eng.* **27** 25–9
[6] X-Ray Mass Attenuation Coefficients. NIST [Internet] 2009 Sep 17 [cited 2023 Jul 17]; Available fromhttps://nist.gov/pml/x-ray-mass-attenuation-coefficients
[7] Thomas S J 1999 Relative electron density calibration of CT scanners for radiotherapy treatment planning *Br. J. Radiol.* **72** 781–6
[8] Sudhyadhom A 2020 On the molecular relationship between Hounsfield Unit (HU), mass density, and electron density in computed tomography (CT) *PLoS One* **15** e0244861
[9] Hughes J, Holloway L C, Quinn A and Fielding A 2012 An investigation into factors affecting electron density calibration for a megavoltage cone-beam CT system *J. Appl. Clin. Med. Phys.* **13** 93–107
[10] Jaafar A M, Elsayed H, Khalil M M, Yaseen M N, Alshewered A and Ammar H 2022 The influence of different kVs and phantoms on computed tomography number to relative electron density calibration curve for radiotherapy dose calculation *Precis. Radiat. Oncol.* **6** 289–97
[11] Park S Y, Choi C H, Park J M, Chun M, Han J H and Kim J 2016 A Patient-Specific Polylactic Acid Bolus Made by a 3D Printer for Breast Cancer Radiation Therapy *PLoS One* ed E Deutsch 11e0168063
[12] Brown K, Kupfer T, Harris B, Penso S, Khor R and Moseshvili E 2022 Not all 3D-printed bolus is created equal: Variation between 3D-printed polylactic acid (PLA) bolus samples sourced from external manufacturers *J. Med. Radiat. Sci.* **69** 348–56
[13] Li X, Lin Y, Liu M, Meng L and Li C 2023 A review of research and application of polylactic acid composites *J. Appl. Polym. Sci.* **140** e53477
[14] Jean M D and Tzeng Y F 2003 Use of taguchi methods and multiple regression analysis for optimal process development of high energy electron beam case hardening of cast iron *Surf. Eng.* **19** 150–6
[15] Kaltrine J, Vladimir D and Atanas K 2022 Analysis of additive manufacturing technology input parameters in manufacturing of bolus *Mech. Eng.-Sci. J.* **40** 17–22
[16] Mutic S *et al* 2003 Quality assurance for computed-tomography simulators and the computed-tomography-simulation process: Report of the AAPM radiation therapy committee task group No. 66 *Med. Phys.* **30** 2762–92
[17] White D R, Booz J, Griffith R V, Spokas J J and Wilson I J 1989 4. The Composition of body tissues *Rep. Int. Comm. Radiat. Units. Meas.* **os-23** 20–3
[18] Semwal M K 2020 Khan's the physics of radiation therapy *J. Med. Phys.* **45** 134–5